Extraordinarily Durable Graphdiyne-Supported Electrocatalyst with High Activity for Hydrogen Production at All Values of pH

Yurui Xue,[†,‡] Jiaofu Li,[‡] Zheng Xue,[†,‡] Yongjun Li,[‡] Huibiao Liu,[‡] Dan Li,[§] Wensheng Yang,*[,†] and Yuliang Li*[,‡]

[†]State Key Laboratory of Supramolecular Structure and Materials, College of Chemistry, Jilin University, Changchun 130012, P.R. China

[‡]Key Laboratory of Organic Solids, Institute of Chemistry, Chinese Academy of Sciences Beijing 100190, P.R. China

[§]Department of Chemistry, Shantou University, Shantou 515063, P.R. China

Ⓢ *Supporting Information*

ABSTRACT: We have used a scalable and inexpensive method to prepare a catalyst comprising graphdiyne nanosheet-supported cobalt nanoparticles wrapped by N-doped carbon (CoNC/GD); this unprecedentedly durable electrocatalyst mediated the hydrogen evolution reaction (HER) with highly catalytic activity over all values of pH. The durability of the CoNC/GD structure was evidenced by the catalytic performance being preserved over 36 000, 38 000, and 9000 cycles under basic, acidic, and neutral conditions, respectively—behavior superior to that of commercial Pt/C (10 wt %) under respective conditions. Such long-term durability has rarely been reported previously for HER catalysts. In addition, this electrode displayed excellent catalytic activity because the improved physical/chemical properties facilitated electron transfer in the composite. The combination of high durability and high activity at all values of pH for this nonprecious metal catalyst suggests great suitability for practical water splitting.

KEYWORDS: *graphdiyne, diacetylenic carbon allotrope, two-dimensional structure, extraordinarily durable, electrocatalyst, hydrogen production*
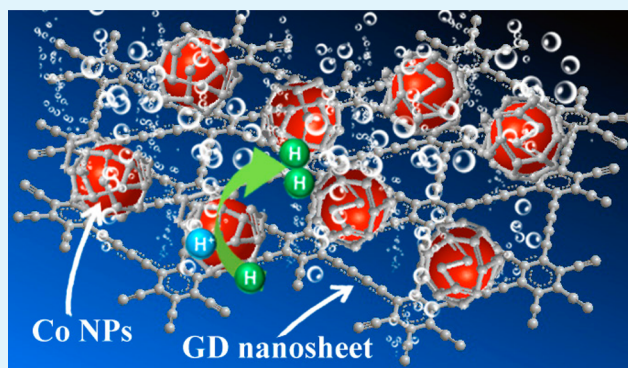
■ INTRODUCTION

The rapid development of clean and sustainable alternative energy has great potential for environmental remediation. Hydrogen gas (H_2) is one of the cornerstones on which energy-dense and renewable clean fuel is based; this energy-dense and renewable clean fuel is a promising candidate for replacing fossil fuels.[1,2] Electrochemical water-splitting, consisting of a hydrogen-evolving reaction (HER) and an oxygen-evolving reaction (OER), is the simplest and most economically viable route for the efficient production of high-purity H_2.[3,4] Although Pt-based catalysts are currently the state-of-the-art for HER, their high cost and scarcity prevent their practical applications. Developing inexpensive catalysts that are not based on noble metals (e.g., transition-metal carbides,[5,6] sulfides,[7−9] selenides,[10] nitrides,[5,11−13] and phosphides[14−17]) for hydrogen production is a great challenge for research into sustainable energy. Ideally, the HER and OER would be conducted in the same electrolyte to ensure an energy-efficient overall water splitting process. In practice, however, most of the current prevailing catalysts for HER exhibit efficient activities only under acidic conditions, whereas the best OER catalysts function well only under alkaline or neutral conditions. Only a very limited number of

catalysts can be operated over a wide pH range, including cobalt phosphide nanowire arrays on carbon cloth (CoP/CC),[15] cobalt-embedded nitrogen-rich carbon nanotubes (Co-NRCNTs),[18] hollow Co-based bimetallic sulfide ($M_xCo_{3−x}S_4$; M = Zn, Ni, Cu) polyhedral,[9] tungsten phosphide nanorod arrays on carbon cloth (WP NAs/CC),[16] and MoP_2 nanoparticles (NPs) on Mo.[17] Despite having decent electrochemical properties, poor durability has restricted the practical applications of these catalysts. Therefore, the challenge remains to develop inexpensive HER electrocatalysts that function over all values of pH with high activity and exceptional stability.

Catalysts based on TMs (e.g., Co) have emerged as alternatives to precious metal catalysts because of their low cost and theoretical activity. Although integration of Co species with carbon materials (e.g., graphene,[19] CNTs[18]) can improve the electrocatalytic properties, the cycle lives of such materials remain limited. Therefore, more suitable supporting materials

 31083

will have to be found to enhance the catalytic performance.[18,20−25]

Graphdiyne (GD), a new carbon allotrope having a one-atom-thick, two-dimensional structure of sp- and sp^2-hybridized carbon atoms, has been predicted to be the most stable diacetylenic carbon allotrope (improved long-term stability under harsh conditions); therefore, it should have high applicability in electronic devices and energy materials.[26−47] The flat sp- and sp^2-hybridized carbon network endows GD with a unique electronic structure and electrical conductivity superior to that of graphene,[48] highly beneficial for electron transfer. Recently, He et al.[49] observed strong chemisorption between TM atoms (e.g., Co) and the alkyne ring of GD, leading to strong electron transfer from, for example, Co to GD, enriching the electron density on the GD shell surface and improving its HER activity. Moreover, the transition metal-adsorbed GD (TM-GD) was proposed to be more stable than corresponding TM-adsorbed graphene, potentially allowing the fabrication of catalysts with more robust long-term durability. In this respect, GD nanosheets would be superior scaffolds for fabricating HER electrocatalysts with excellent long-term durability and catalytic activity. Despite tremendous interest in GD, to the best of our knowledge, no previous reports have appeared regarding the use of GD-based electrocatalysts for HER.

In this paper, we report a scalable and inexpensive method for preparing GD-supported Co NPs wrapped by N-doped carbon layers (denoted "CoNC/GD"; Scheme 1, see

Scheme 1. Schematic Representation of the Fabrication of the CoNC/GD. Synthesis Steps: (1) Adsorption of Co(oAc)$_2$ and DCD onto GD Nanosheets; (2) Sequential Annealing Treatments of the Mixture at 500 and 700 °C in Ar Atmosphere; (3) Additional Acid Treatment of the Resulting Materials
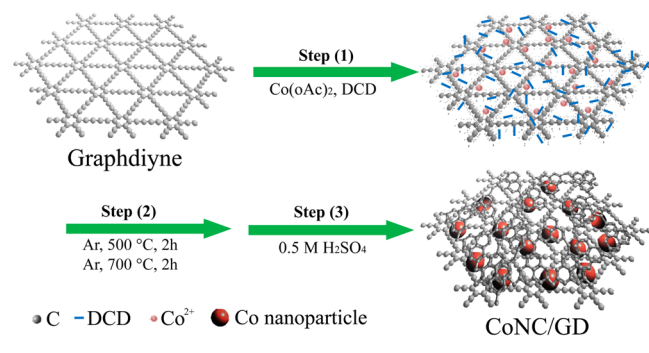
Experimental Section for details). This is the first GD-based HER electrocatalyst that functions well at all values of pH. The composite cathode exhibited unprecedented durability; for example, its HER catalytic activity was preserved for 36 000, 38 000, and 9000 cycles under basic, acidic, and neutral conditions, respectively, surpassing that of commercial Pt/C (10 wt %) under respective conditions. The unique architecture also improved the physical/chemical properties, thereby increasing its electron transfer ability and resulting in high catalytic activity. To the best of our knowledge, such excellent long-term stability for a non-noble-metal HER catalyst that can be operated at all values of pH has never been reported previously.

EXPERIMENTAL SECTION

Materials. Tetrabutylammonium fluoride (TBAF) was purchased from Alfa Aesar. Hexabromobenzene was obtained from J&K Scientific. Commercial Pt/C (10 wt % Pt on an activated carbon support) was purchased from Alfa Aesar. Toluene and tetrahydrofuran (THF) were pretreated by drying under reflux with Na crumbs. Unless otherwise specified, all other reagents were purchased commercially from Sinopharm Chemical Reagent and used without further purification. All aqueous solutions were prepared with Milli-Q water.

Preparation of GD. GD was synthesized on the surface of copper using a modified Glaser−Hay coupling reaction using hexaethynyl-benzene (HEB) precursors, as described previously.[29] In a typical procedure, HEB was first synthesized by adding TBAF (1 M in THF, 1.2 mmol) to a THF solution of hexakis[(trimethylsilyl)ethynyl]-benzene (0.20 mmol) at 0 °C for 10 min. The solution was then mixed with ethyl acetate, followed by being extracted with saturated sodium chloride solution for three times and dried by anhydrous Na$_2$SO$_4$. The solvent was removed under reduced pressure. The obtained HEB was immediately dissolved in pyridine (25 mL) and added very slowly into a solution of Cu foil in pyridine (50 mL) at 80 °C. In the process of GD formation, the Cu foil served as not only the catalyst for the cross-coupling reaction but also the substrate for the growth of the GD film. The mixture was then heated for 3 days at 80 °C under a N$_2$ atmosphere, protected from light. Upon completion of the reaction, the Cu foils covered by GD layers were washed with hot acetone and DMF under sonication for 1 h to obtain a black solid, which was then thoroughly washed sequentially with 4 M NaOH, 6 M HCl, and 4 M NaOH to remove impurities. Finally, the black solid was collected by centrifugation; washed sequentially with Milli-Q water, hot DMF (80 °C), and acetone; and dried in a vacuum oven at 60 °C. The resulting pure bulk GD was exfoliated under sonication for 2 weeks to form a homogeneous aqueous dispersion of GD.

Preparation of CoNC/GD. Cobalt acetate tetrahydrate [Co-(CH$_3$COO)$_2$·4H$_2$O, 0.80 mmol] and Dicyandiamide (DCD, C$_2$H$_4$N$_4$, 1.2 mmol) were codissolved in ethanol/water (1:1, v/v; 20 mL). The mixture was then heated at 80 °C with vigorous stirring for 5 h. A GD suspension (2 mg/mL, 3 mL) was added to the mixture, which was then stirred for 5 h. The homogeneous mixture was rotary evaporated to dryness. Finely ground samples were placed on a covered alumina boat and then heated (with a ramp of 10 °C/min) at 500 °C for 2 h and then at 700 °C for 2 h under a N$_2$ atmosphere. The resultant black powder was treated with 0.5 M H$_2$SO$_4$, washed thoroughly with distilled water, and dried under vacuum.

For comparison, samples were also prepared using a similar procedure but without the addition of Co(CH$_3$COO)$_2$·4H$_2$O or DCD; these samples are denoted "NC/GD" and "Co/GD," respectively.

Characterization. Scanning electron microscopy (SEM) images were recorded using a Hitachi Model S-4800 field emission scanning electron microscope. TEM and HRTEM were performed using a JEM-2100F electron microscope with an accelerating voltage of 200 kV. XPS was performed using a Thermo Scientific ESCALab 250Xi instrument and 200-W monochromated Al Kα radiation. The binding energies obtained in the XPS analyses were corrected with reference to C 1s (284.8 eV). XRD data were collected using a Japan Rigaku D/max-2500 rotation anode X-ray diffractometer and graphite-mono-chromated Cu Kα radiation (λ = 1.54178 Å). Raman spectra were recorded at a resolution of 2 cm^{-1} using a Renishaw-2000 Raman spectrometer, with the 514.5 nm line of an Ar ion laser as the excitation source. BET surface areas were measured using a Micromeritics ASAP 2020 HD88 system with N$_2$ adsorption at 77 K and the Barrett−Joyner−Halenda (BJH) method. The Brunauer−Emmett−Teller (BET) surface area and the pore size distribution of the catalysts were measured using a Micromeritics ASAP 2020 HD88 system and the Barrett−Joyner−Halenda (BJH) method. All the samples were degassed at 150 °C prior to measurements.

Electrochemical Measurements. Electrocatalytic properties were studied using an electrochemical workstation (CHI. 660D, Shanghai CH. Instruments, China) with a typical three-electrode system. A
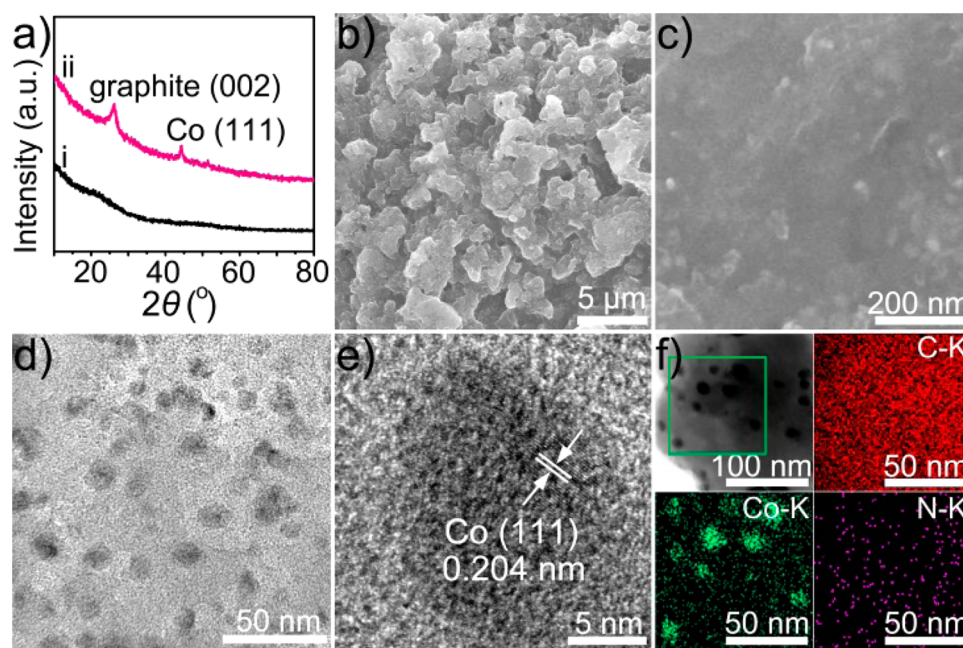
Figure 1. (a) XRD patterns of (i) GD and (ii) CoNC/GD, indicating the characteristic peaks for graphite and metallic Co. (b, c) SEM images of CoNC/GD at (b) low and (c) high magnification. (d) TEM and (e) HRTEM images of CoNC/GD. (f) STEM image and EDX elemental mapping of C, Co, and N for the CoNC/GD catalyst.
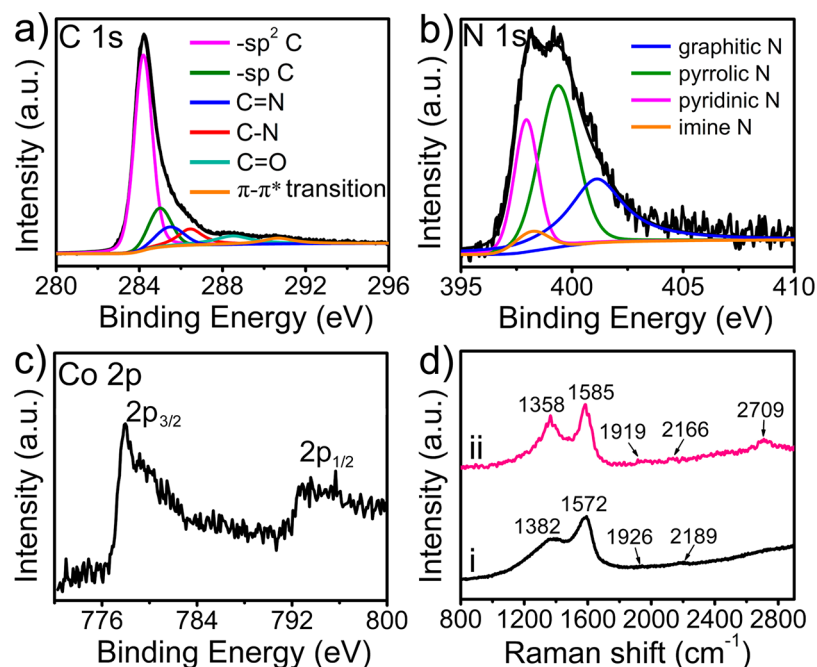

Figure 2. High-resolution XPS spectra of CoNC/GD: (a) C 1s, (b) N 1s, (c) Co 2p. (d) Raman spectra of pristine GD (trace i) and CoNC/GD (trace ii).

saturated calomel electrode (SCE) was used as the reference electrode and a carbon rod as the counter electrode. To prepare the catalyst ink, the catalyst (1 mg) was mixed with ethanol/water (1:1, v/v; 960 μL) and 5 wt % Nafion solution (40 μL) under sonication for 2 h. A portion (20 μL) of the above solution was then drop-cast onto the surface of a GCE and dried at room temperature, yielding a catalyst loading of approximately 0.286 mg cm^{-2}. Linear sweep voltammetry (LSV) of CoNC/GD (scan rate: 5 mV/s) was performed at room temperature in 0.5 M H$_2$SO$_4$ (pH 0), 1 M PBS (pH 7), or 1 M KOH (pH 14). CV was conducted at a scan rate of 100 mV s^{-1}. All potentials (E), measured against the SCE electrode, were converted to

the reversible hydrogen electrode (RHE) scale, according to the equation: E (versus RHE) = E (versus SCE) + E^0 (SCE) + 0.059pH. The electrochemical impedance spectra (EIS) were performed with the working electrode at a certain potential in the frequency from 100 kHz to 1 Hz with a sampling rate of 12 points per decade. A Nyquist plot was recorded to analyze the impedance results.

■ RESULTS AND DISCUSSION

The crystal structures of pristine GD and CoNC/GD were examined using X-ray diffraction (XRD, Figure 1a). Compared to pristine GD, the CoNC/GD (Figure 1a, trace (ii) shows a
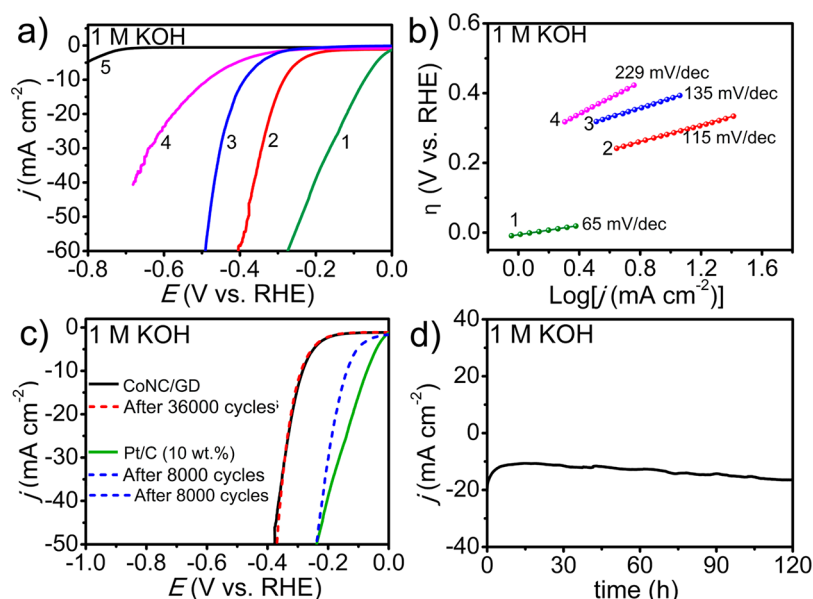
Figure 3. (a) HER polarization curves and (b) corresponding Tafel plots in 1 M KOH (pH 14). (c) HER polarization curves of CoNC/GD and commercial Pt/C (10 wt %) before and after 36 000 and 8000 CV scans, respectively, in 1 M KOH at a scan rate of 100 mV s^{-1} between −1.0 and −1.4 V. (d) Current density−time curve for CoNC/GD at an overpotential of 362 mV for 120 h in 1 M KOH. Sample labels: 1, 10 wt % Pt/C; 2, CoNC/GD; 3, Co/GD; 4, NC/GD; 5, pristine GD.

broad peak located around 25.5°, corresponding to the (002) plane of graphite-type carbon. The characteristic peaks located around 44.2 and 51.5° correspond to the (111) crystal planes of face-centered cubic (fcc)−structured metallic Co (JCPDS No. 15−0806).[50] These observations revealed the success formation of Co−C−GD composites. SEM images (Figure 1b and c) revealed the three-dimensional (3D) macroporous interconnected features of the CoNC/GD catalyst and the rough surface morphology of the GD sheets, resulting from the presence of the Co NPs. The porosity of CoNC/GD was demonstrated in nitrogen (N$_2$) adsorption/desorption isotherms (Figure S1a). The N$_2$ isotherm for CoNC/GD featured an intermediate mode between type I and type IV isotherms with a steep N$_2$ uptake at low relative pressure (P/P_0) and a steep hysteresis loop at relative pressures ranging from 0.4 to 1.0, suggesting a micro/mesoporous structure. The pore size distribution curves revealed that the pore sizes of the CoNC/GD were centered mainly in the range 1−9 nm (Figure S1b). A hierarchical porosity and pore size is an important aspect for catalytic applications of such materials. The Brunauer− Emmett−Teller (BET) surface area of CoNC/GD was calculated to be approximately 104.0 m^2/g. The transmission electron microscopy (TEM) image observed at low magnification (Figure 1d) revealed many small Co NPs uniformly dispersed on the surface of the GD sheets. The size distribution of the Co NPs exhibits a most probable diameter of ∼7.58 nm as calculated by Gaussian fitting (Figure S2). The high-resolution TEM (HRTEM) image (Figure 1e) revealed the presence of crystallized Co NPs having an interplanar spacing of 0.204 nm, consistent with the (111) plane of fcc Co. Furthermore, the scanning TEM (STEM) image and corresponding energy dispersive X-ray (EDX) elemental mapping images of CoNC/GD (Figure 1f) revealed the presence of C, Co, N, and O (not shown) atoms, and the discrete dispersion of the Co NPs in accordance with the TEM image in Figure 1d.

X-ray photoelectron spectroscopy (XPS) was performed to determine the chemical composition and elemental states of the CoNC/GD. The survey spectrum (Figure S3) of CoNC/GD revealed the characteristic peaks of C, N, O, and Co atoms, in accordance with the EDX data (Figure 1f). We ascribe the presence of an O 1s peak at 532 eV to the absorption of air. As displayed in Figure 2a, the C 1s peak can be deconvoluted into five subpeaks. The component peaks at 284.2 and 285.0 eV are assigned to the C 1s orbitals of C−C (sp^2) and C−C (sp) atoms, respectively.[51] The peaks centered at 285.5 and 286.4 eV are ascribed to sp^2-type C=N bonds and sp^3-type C−N bonds,[52] whereas the peak at 288.5 eV corresponds to C=O bonds, arising from adsorption of O$_2$ from the atmosphere.[29] The shakeup satellite peak at 290.6 eV represents the π−π* transitions of the aromatic rings. The XPS N 1s spectrum (Figure 2b) was fitted to different types of N species at 397.9, 398.2, 399.4, and 401.1 eV, which could be assigned to pyridinic-N, imine-N (minor N substitution of the sp-hybridized carbon atoms), pyrrolic-N, and graphitic-N species, respectively.[53] According to previous literature, the peaks of imine-N or pyridinic-N may also originate from N-doped GD network.[54] These types of N atoms in CoNC/GD may serve as electrocatalytically active sites for HER. The high-resolution Co 2p spectrum (Figure 2c) features two peaks at 777.9 and 793.4 eV, corresponding to the Co 2p$_{3/2}$ and Co 2p$_{1/2}$ orbitals of metallic Co, respectively. This observation is also consistent with the powder XRD and TEM data and confirms the successful synthesis of the CoNC/GD composite electrode.

Detailed structural information on samples was obtained using Raman spectroscopy. Figure 2d presents the Raman spectra of pristine GD and CoNC/GD. In agreement with previous reports, the spectrum of the pristine GD (Figure 2d, trace i) featured D and G bands at 1382 and 1572 cm^{-1}, with peaks at 1926 and 2189 cm^{-1} corresponding to vibrations of the conjugated diyne links (−C≡C−C≡C−).[29,55] The Raman spectrum of CoNC/GD (Figure 2d, trace ii) features five prominent peaks. We assign the signals at 1358 and 1585 cm^{-1}
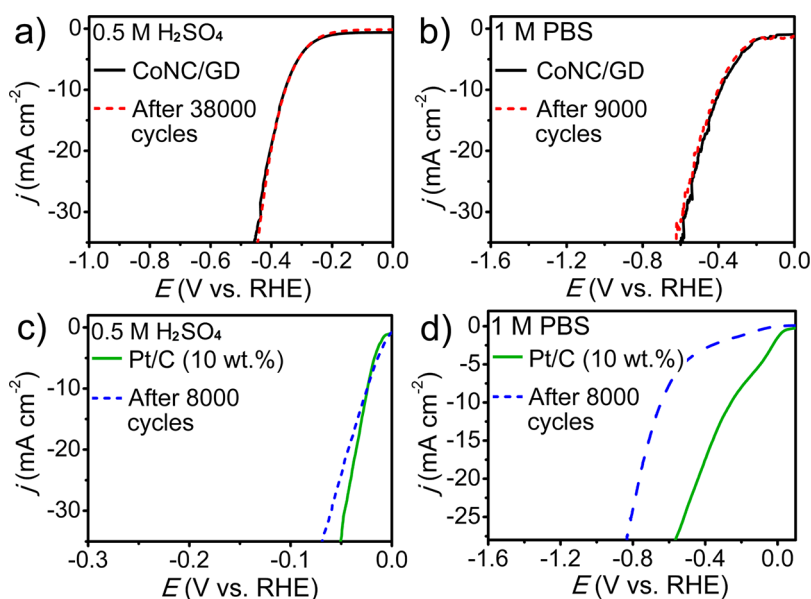
Figure 4. HER polarization curves of CoNC/GD in (a) 0.5 M H_2SO_4 initially and after 38 000 CV scans and (b) 1 M PBS initially and after 9000 CV scans. HER polarization curves of commercial Pt/C (10 wt %) before and after 8000 CV scans in (c) 0.5 M H_2SO_4 and (d) 1 M PBS.

to the D and G bands, and those at 1919 and 2166 cm^{-1} to the vibrations of the conjugated diyne links. These observations suggest that the GD substrates remained undamaged after the high-temperature treatment. The peak located at 2709 cm^{-1} corresponds to the 2D band of the C shells. Compared with the spectrum of the pristine GD, a slight blue-shifting had occurred to the signals for the vibrations of the conjugated diyne links, reflecting the formation of chemical bonds between the GD and the Co NPs; such bonds would effectively increase the electron transfer ability and, thereby, improve the device's electronic properties.[37,56,57] The ratio of the intensities of the D and G bands (I_D/I_G) is typically used to reflect the degree of graphitization or defect density in carbon materials.[58] The I_D/I_G ratio of the CoNC/GD (0.94) was larger than that of the pristine GD (0.73), indicating that many more structural defect sites existed in it along with a higher degree of disorder. This observation implies that CoNC/GD had more active sites exposed for electrocatalysis than did the pristine GD.

We used a typical three-electrode system to evaluate the electrochemical performance of CoNC/GD over a wide range of pH at a scan rate of 5 mV/s; a GCE modified with the catalyst was used as the working electrode (mass loading: 0.286 mg/cm). The electrocatalytic activities of commercial Pt/C (10 wt %), Co/GD, NC/GD, and pristine GD were examined for comparison. Potentials are reported versus the reversible hydrogen electrode (RHE).

Figure 3a displays polarization curves of CoNC/GD in 1 M KOH (pH 14) with *iR* compensation. As expected, Pt/C (10 wt %) displayed the best HER activity with a near-zero onset potential. CoNC/GD had a remarkably high HER activity with an onset potential of 170 mV, lower than those of Co/GD (260 mV), NC/GD (300 mV), and pristine GD (700 mV), suggesting higher electrocatalytic activity for CoNC/GD. The excellent catalytic activity of CoNC/GD was confirmed by its current density being higher than those of the other samples over the whole potential range. Notably, the current density of CoNC/GD was higher than that of Pt/C (10 wt %) when the applied potential exceeded 406 mV, suggesting that the catalytic activity for CoNC/GD was higher than that for Pt/C.

According to these results, the catalytic activities of both Co/GD and NC/GD were higher than that of pristine GD, implying that both the Co species and the N-rich C species were beneficial to the HER activity of CoNC/GD. In addition, the onset potential of Co/GD is more positive than that of NC/GD; this value should be the main contributor to the HER activity. CoNC/GD required overpotentials of 284 and 315 mV to achieve current densities of 10 and 20 mA/cm^2, respectively. These values compare favorably with those of many recently reported HER catalysts in alkaline electrolytes (Table S1).

The electrocatalytic performance of the as-prepared catalysts in 1 M KOH was further characterized by electrochemical impedance spectroscopy (EIS, Figure S4). The Nyquist plots for all samples can be fit with an equivalent circuit model, which has been widely used to simulate the HER kinetics of the catalysts.[59,60] This model was built using series components, including R_s (the uncompensated solution resistance), CPE_1 (related to the double layer capacitance), and R_{ct} (catalytic charge-transfer resistance). The parameters obtained by fitting the EIS spectra to equivalent circuit model were summarized in Table S6. Among the as-prepared catalysts, the smallest equivalent series resistance (R_s, 10.03 Ω) and charge transfer resistance (R_{ct}, 27.49 Ω) values of CoNC/GD confirms that the CoNC/GD electrode is the most active for the HER.

To gain insight into the kinetics of the HER process, we recorded Tafel plots with the linear portions fitted to the Tafel equation ($\eta = b \log j + a$) where j is the current density and b is the Tafel slope. Figure 3b reveals that CoNC/GD provided a Tafel slope (115 mV/dec) lower than those for Co/GD (135 mV/dec) and NC/GD (229 mV/dec), and lower than those of cobalt phosphide nanowire arrays/carbon cloth (129 mV/dec),[15] EG/Co0.85Se/NiFe-LDH (160 mV/dec),[61] NiCo$_2$S$_4$ nanowire array/carbon cloth (141 mV/dec),[62] and NiCo-LDH/Ni foam (124.2 mV/dec).[63] Its value compare favorably to those of many recently reported HER catalysts in alkaline electrolytes (Table S1). Because the Tafel value for CoNC/GD is in the range 40−120 mV/dec, the HER proceeds through a Volmer−Heyrovsky mechanism under alkaline conditions.[64]

In addition to its catalytic activity, the long-term durability is a critical challenge affecting the practical applications of any electrocatalyst. As revealed in Figure 3c, the polarization curve of the CoNC/GD recorded after continuous cyclic voltammetry (CV) scanning for 36,000 cycles remained almost identical to its initial curve. In contrast, the commercial Pt/C (10 wt %) underwent an obvious loss of activity in the low current density range after only 8000 cycles. Thus, the durability of CoNC/GD was much greater than that of Pt/C for long-term electrochemical HER processing in alkaline electrolytes. We suspect that the robust protection that precluded exposure of the inner-core materials to the electrolyte was mostly responsible for this excellent durability. To the best of our knowledge, HER catalysts displaying such excellent long-term durability have never been reported before. We performed a chronoamperometry test at an overpotential of 362 mV for 120 h in 1 M KOH to confirm the stability of the CoNC/GD catalyst (Figure 3d). The slight decrease in current density observed during the initial period might have been due to the reduced active sites occupied by physical adsorption of the H_2 bubbles generated on the electrode surface. Thereafter, the current density increased slowly, possibly because of a surface roughening effect.[65] Compared with other HER electrocatalysts (Table S2), the high activity and robust long-term durability indicate that CoNC/GD is an excellent catalyst for HER under alkaline conditions.

Next, we studied the HER performance of CoNC/GD in 0.5 M H_2SO_4. This electrode displayed high activity with a low onset potential of 190 mV (Figure 4a), beyond which the cathodic current density rose rapidly under more negative potentials; in contrast, Co/GD, NC/GD, and the pristine GD displayed inferior potentials of 360, 380, and 500 mV, respectively (Figure S6a). Both Co/GD and NC/GD had catalytic activities higher than that of the pristine GD, implying that both the Co atoms and NC were the active centers for HER. The fact that the onset potential of NC/GD was more negative than that of Co/GD further demonstrated that Co/GD provided the main active centers for CoNC/GD. The electrocatalytic performance of the as-prepared catalysts was further characterized by EIS (Figure S5) and the parameters obtained by fitting the EIS spectra to equivalent circuit model were summarized in Table S7. The smallest R_{ct} (31.5 Ω) indicates the fastest charge-transfer kinetics over the CoNC/GD-electrolyte interface, confirming the fact that CoNC/GD is the most active for the HER. The Tafel slope calculated from the Tafel plots of CoNC/GD was 138 mV/dec (Figure S6b), superior to those of Co/GD (184 mV/dec) and NC/GD (259 mV/dec), indicating more favorable HER kinetics for CoNC/GD. Notably, CoNC/GD also exhibited strong durability in 0.5 M H_2SO_4, as evidenced using CV. Figure 4a reveals that there was almost no difference in catalytic activity before and after 38,000 cycles. In contrast, a non-negligible decrease in catalytic activity occurred for the commercial Pt/C (10 wt %) after only 8000 cycles. A chronoamperometric test of CoNC/GD for 100 h verified its reliable stability (Figure S7). Thus, CoNC/GD also displayed excellent durability in an acidic electrolyte. Its behavior is vastly superior to that of the state-of-the-art commercial Pt/C (10 wt %) (Figure 4c) and many other recently reported HER catalysts not based on noble metals (Table S3).

Performing HER under neutral media is generally regarded as a more environmentally friendly and low-cost approach for water splitting.[66,67] Therefore, after studying the effects of both alkaline and acidic media, the electrochemical performance of CoNC/GD was further investigated under a neutral medium (1 M PBS, pH 7). In accordance with the behavior in both alkaline and acidic conditions, the catalytic activity of CoNC/GD was again higher than that of Co/GD, NC/GD, and pristine GD in the neutral medium (Figure S8a). Interestingly, the current density of CoNC/GD was higher than that of the commercial Pt/C when the applied potential exceeded 400 mV, indicating a higher catalytic activity for CoNC/GD than for Pt/C. CoNC/GD exhibited an onset overpotential of 160 mV (Figure 4b) and a Tafel slope of 207 mV/dec (Figure S8b). Driving current densities of 10 and 20 mA/cm² required overpotentials of 368 and 478 mV, respectively (Figure 4b). These values also compare favorably to many of the reported values for non-noble-metal HER catalysts in neutral electrolytes (Table S4). The EIS data was determined and simulated by an equivalent circuit model (Figure S9). As can be seen from the parameters obtained by fitting the EIS spectra (Table S8), the CoNC/GD exhibits the smallest R_{ct} (22.69 Ω) in 1 M PBS, indicating more favorable HER kinetics for CoNC/GD. Again, CoNC/GD displayed unprecedented durability under the neutral conditions. After continuous CV scanning for 9000 cycles in 1 M PBS, the polarization curve revealed a negligible loss in catalytic activity when compared with that recorded initially (Figure 4b). In contrast, the commercial Pt/C (10 wt %) displayed an obvious decay in catalytic activity after only 8000 cycles (Figure 4d). This finding confirms the exceptional durability of CoNC/GD for HER under neutral conditions; it is superior not only to the state-of-the-art commercial Pt/C (10 wt %) but also many previously reported non-noble-metal based HER catalysts (Table S5). A chronoamperometry test performed at an overpotential of 465 mV (Figure S10) revealed that CoNC/GD could maintain its catalytic activity for at least 18 h, confirming its long-term stability under neutral conditions. These results make CoNC/GD among the most active and durable HER catalysts based on earth-abundant elements for operation under neutral conditions. Taken together, CoNC/GD exhibits high catalytic performance, and especially exceptional durability, for HER at all values of pH.

Strong chemisorption can occur between transition metals (e.g., Co) and the alkyne rings of GD,[49] allowing ready access of cobalt precursors to facilitate the deposition of Co NPs on GD nanosheets (Co/GD). This interaction also leads to stronger electron transfer from Co to GD, enriching the electron density on the GD surface and, thereby, promoting hydrogen adsorption and evolution.[68] Providing a carbon coating on the surface of Co/GD can not only protect the Co NPs from corrosion by the electrolyte but also prevent them from coalescing, leading to robust performance and long-term stability. In addition, heteroatom-doped graphitic carbon materials can certainly provide a number of active sites for HER. The approach described herein appears to be a practical strategy for the fabrication of GD-based hybrid composites for versatile applications.

In general, Co metal is an unstable catalyst, especially in acidic solutions, restricting its applications in HER. In this study, CoNC/GD exhibited excellent stability over all values of pH; its stability is even greater than that of commercial Pt/C. The significant enhancement in durability suggests that CoNC/GD electrodes may be more applicable in energy generation. Such electrodes benefit from four main properties: (i) the unique electronic structure and high conductivity of the GD nanosheets makes them highly conductive supporting matrices;

(ii) the high porosity of the GD structure and the well-defined macro/mesoporosity of the catalyst, demonstrated by N_2 adsorption experiments, facilitate efficient mass transport, leading to more efficient use of active sites; (iii) the Co atoms are inclined to interact with the alkyne rings, facilitating rapid electron transfer from Co atoms to the GD sheets, enriching the electron density on the GD shell surface and, thereby, improving the HER activity, as experimentally observed; in addition, confinement of the Co NPs in the hybrid catalyst protects the Co atoms from corrosion and aggregation, enhancing the durability of the catalyst; in contrast, Co/GD displayed poor HER performance (Figures 3a and 4a, b); (iv) the intimate contacts of the Co atoms with both the GD nanosheets and the N-doped carbon coatings not only provided more catalytically active sites but also greatly enhanced the long-term stability of the catalysts.

CONCLUSIONS

The first GD-supported electrocatalyst (CoNC/GD) that functions over a wide pH range has been prepared through a simple, scalable synthetic route involving reduction of Co^{2+} and simultaneous decomposition of Dicyandiamide. The composite exhibited unprecedented durability, far superior to that of a commercial Pt/C (10 wt %) under respective conditions. The long-term durability demonstrated herein has rarely been reported for other HER catalysts. The enhanced catalytic performance of CoNC/GD resulted from the improved physical/chemical properties, which facilitated electron transfer, in the composite. The combination of remarkable durability and high activity over a wide pH range is rare for a nonprecious-metal catalyst and suggests high applicability in practical water splitting devices. This study has not only afforded a convenient and scalable method toward GD-based electrocatalysts but also paves a new path toward the practical industrialization of devices for sustainable energy-related applications.

ASSOCIATED CONTENT

Ⓢ Supporting Information

The Supporting Information is available free of charge on the ACS Publications website at DOI: 10.1021/acsami.6b12655.

> BET, XPS, Nyquist plots, HER polarization curves, Tafel plots, and current density-time curves of samples; comparison of the HER activity of the CoNC/GD with recently reported in literatures (PDF)

AUTHOR INFORMATION

Corresponding Authors
*E-mail: wsyang@jlu.edu.cn.
*E-mail: ylli@iccas.ac.cn.

Author Contributions
Y.L. (Yuliang Li) conceived, designed, and supervised the project; analyzed the data; and revised the paper. W.Y. supervised the experiment. Y.X. performed all experiments, analyzed the data, and wrote the paper. Y.L. (Yongjun Li) helped in analyzing data and revising the paper. J.L. contributed to the synthesis of GD. Z.X. helped in characterizing the samples. H.L. and D.L. helped in analyzing data. All authors have given approval to the final version of the manuscript.

Notes
The authors declare no competing financial interest.

REFERENCES

(1) Lubitz, W.; Ogata, H.; Rüdiger, O.; Reijerse, E. Hydrogenases. *Chem. Rev.* **2014**, *114*, 4081−4148.

(2) Rand, D. A. J.; Dell, R. M.*Hydrogen Energy: Challenges and Prospects*; RSC Publishing: Cambridge, U.K., 2007; DOI: 10.1039/9781847558022.

(3) Turner, J. A. Sustainable Hydrogen Production. *Science* **2004**, *305*, 972−974.

(4) Walter, M. G.; Warren, E. L.; McKone, J. R.; Boettcher, S. W.; Mi, Q.; Santori, E. A.; Lewis, N. S. Solar Water Splitting Cells. *Chem. Rev.* **2010**, *110*, 6446−6473.

(5) Chen, W.-F.; Muckerman, J. T.; Fujita, E. Recent Developments in Transition Metal Carbides and Nitrides as Hydrogen Evolution Electrocatalysts. *Chem. Commun.* **2013**, *49*, 8896−8909.

(6) Tuomi, S.; Guil-Lopez, R.; Kallio, T. Molybdenum Carbide Nanoparticles as a Catalyst for the Hydrogen Evolution Reaction and the Effect of pH. *J. Catal.* **2016**, *334*, 102−109.

(7) Faber, M. S.; Dziedzic, R.; Lukowski, M. A.; Kaiser, N. S.; Ding, Q.; Jin, S. High-Performance Electrocatalysis Using Metallic Cobalt Pyrite (CoS_2) Micro- and Nanostructures. *J. Am. Chem. Soc.* **2014**, *136*, 10053−10061.

(8) Hinnemann, B.; Moses, P. G.; Bonde, J.; Jørgensen, K. P.; Nielsen, J. H.; Horch, S.; Chorkendorff, I.; Nørskov, J. K. Biomimetic Hydrogen Evolution: MoS_2 Nanoparticles as Catalyst for Hydrogen Evolution. *J. Am. Chem. Soc.* **2005**, *127*, 5308−5309.

(9) Huang, Z.; Song, J.; Li, K.; Tahir, M.; Wang, Y.-T.; Pan, L.; Wang, L.; Zhang, X.; Zou, J. Hollow Cobalt-Based Bimetallic Sulfide Polyhedra for Efficient All-pH-Value Electrochemical and Photocatalytic Hydrogen Evolution. *J. Am. Chem. Soc.* **2016**, *138*, 1359−1365.

(10) Liu, Q.; Shi, J.; Hu, J.; Asiri, A. M.; Luo, Y.; Sun, X. $CoSe_2$ Nanowires Array as a 3D Electrode for Highly Efficient Electrochemical Hydrogen Evolution. *ACS Appl. Mater. Interfaces* **2015**, *7*, 3877−3881.

(11) Chen, W.-F.; Sasaki, K.; Ma, C.; Frenkel, A. I.; Marinkovic, N.; Muckerman, J. T.; Zhu, Y.; Adzic, R. R. Hydrogen-evolution Catalysts based on Non-noble Metal Nickel−Molybdenum Nitride Nanosheets. *Angew. Chem., Int. Ed.* **2012**, *51*, 6131−6135.

(12) Wang, T.; Wang, X.; Liu, Y.; Zheng, J.; Li, X. A Highly Efficient and Stable Biphasic Nanocrystalline Ni−Mo−N Catalyst for Hydrogen Evolution in Both Acidic and Alkaline Electrolytes. *Nano Energy* **2016**, *22*, 111−119.

(13) Zhang, Y.; Ouyang, B.; Xu, J.; Chen, S.; Rawat, R. S.; Fan, H. J. 3D Porous Hierarchical Nickel−Molybdenum Nitrides Synthesized by RF Plasma as Highly Active and Stable Hydrogen-evolution-reaction Electrocatalysts. *Adv. Energy Mater.* **2016**, *6*, 1600221.

(14) Popczun, E. J.; Read, C. G.; Roske, C. W.; Lewis, N. S.; Schaak, R. E. Highly Active Electrocatalysis of the Hydrogen Evolution Reaction by Cobalt Phosphide Nanoparticles. *Angew. Chem., Int. Ed.* **2014**, *53*, 5427−5430.

(15) Tian, J.; Liu, Q.; Asiri, A. M.; Sun, X. Self-Supported Nanoporous Cobalt Phosphide Nanowire Arrays: An Efficient 3D Hydrogen-Evolving Cathode over the Wide Range of pH 0−14. *J. Am. Chem. Soc.* **2014**, *136*, 7587−7590.

(16) Pu, Z.; Liu, Q.; Asiri, A. M.; Sun, X. Tungsten Phosphide Nanorod Arrays Directly Grown on Carbon Cloth: A Highly Efficient and Stable Hydrogen Evolution Cathode at All pH Values. *ACS Appl. Mater. Interfaces* **2014**, *6*, 21874−21879.

(17) Pu, Z.; Saana Amiinu, I.; Wang, M.; Yang, Y.; Mu, S. Semimetallic MoP_2: an Active and Stable Hydrogen Evolution

Electrocatalyst over the Whole pH Range. *Nanoscale* **2016**, *8*, 8500−8504.

(18) Zou, X.; Huang, X.; Goswami, A.; Silva, R.; Sathe, B. R.; Mikmeková, E.; Asefa, T. Cobalt-Embedded Nitrogen-Rich Carbon Nanotubes Efficiently Catalyze Hydrogen Evolution Reaction at All pH Values. *Angew. Chem., Int. Ed.* **2014**, *53*, 4372−4376.

(19) Zhou, W.; Zhou, J.; Zhou, Y.; Lu, J.; Zhou, K.; Yang, L.; Tang, Z.; Li, L.; Chen, S. N-Doped Carbon-wrapped Cobalt Nanoparticles on N-Doped Graphene Nanosheets for High-efficiency Hydrogen Production. *Chem. Mater.* **2015**, *27*, 2026−2032.

(20) Fei, H.; Dong, J.; Arellano-Jiménez, M. J.; Ye, G.; Dong Kim, N.; Samuel, E. L. G.; Peng, Z.; Zhu, Z.; Qin, F.; Bao, J.; Yacaman, M. J.; Ajayan, P. M.; Chen, D.; Tour, J. M. Atomic Cobalt on Nitrogen-doped Graphene for Hydrogen Generation. *Nat. Commun.* **2015**, *6*, 8668.

(21) Fei, H.; Yang, Y.; Peng, Z.; Ruan, G.; Zhong, Q.; Li, L.; Samuel, E. L. G.; Tour, J. M. Cobalt Nanoparticles Embedded in Nitrogen-doped Carbon for the Hydrogen Evolution Reaction. *ACS Appl. Mater. Interfaces* **2015**, *7*, 8083−8087.

(22) Li, X.; Niu, Z.; Jiang, J.; Ai, L. Cobalt Nanoparticles Embedded in Porous N-rich Carbon as an Efficient Bifunctional Electrocatalyst for Water Splitting. *J. Mater. Chem. A* **2016**, *4*, 3204−3209.

(23) Xiao, M.; Zhu, J.; Feng, L.; Liu, C.; Xing, W. Meso/Macroporous Nitrogen-Doped Carbon Architectures with Iron Carbide Encapsulated in Graphitic Layers as an Efficient and Robust Catalyst for the Oxygen Reduction Reaction in Both Acidic and Alkaline Solutions. *Adv. Mater.* **2015**, *27*, 2521−2527.

(24) Zhu, J.; Xiao, M.; Zhao, X.; Liu, C.; Ge, J.; Xing, W. Strongly Coupled Pt Nanotubes/N-doped Graphene as Highly Active and Durable Electrocatalysts for Oxygen Rreduction Reaction. *Nano Energy* **2015**, *13*, 318−326.

(25) Xing, Z.; Liu, Q.; Xing, W.; Asiri, A. M.; Sun, X. Interconnected Co-Entrapped, N-Doped Carbon Nanotube Film as Active Hydrogen Evolution Cathode over the Whole pH Range. *ChemSusChem* **2015**, *8*, 1850−1855.

(26) Qi, H.; Yu, P.; Wang, Y.; Han, G.; Liu, H.; Yi, Y.; Li, Y.; Mao, L. Graphdiyne Oxides as Excellent Substrate for Electroless Deposition of Pd Clusters with High Catalytic Activity. *J. Am. Chem. Soc.* **2015**, *137*, 5260−5263.

(27) Zhang, S.; Liu, H.; Huang, C.; Cui, G.; Li, Y. Bulk Graphdiyne Powder Applied for Highly Efficient Lithium Storage. *Chem. Commun.* **2015**, *51*, 1834−1837.

(28) Srinivasu, K.; Ghosh, S. K. Graphyne and Graphdiyne: Promising Materials for Nanoelectronics and Energy Storage Applications. *J. Phys. Chem. C* **2012**, *116*, 5951−5956.

(29) Li, G.; Li, Y.; Liu, H.; Guo, Y.; Li, Y.; Zhu, D. Architecture of Graphdiyne Nanoscale Films. *Chem. Commun.* **2010**, *46*, 3256−3258.

(30) Diederich, F.; Kivala, M. All-Carbon Scaffolds by Rational Design. *Adv. Mater.* **2010**, *22*, 803−812.

(31) Rivera-Fuentes, P.; Diederich, F. Allenes in Molecular Materials. *Angew. Chem., Int. Ed.* **2012**, *51*, 2818−2828.

(32) Li, Y.; Xu, L.; Liu, H.; Li, Y. Graphdiyne and Graphyne: From Theoretical Predictions to Practical Construction. *Chem. Soc. Rev.* **2014**, *43*, 2572−2586.

(33) Thangavel, S.; Krishnamoorthy, K.; Krishnaswamy, V.; Raju, N.; Kim, S. J.; Venugopal, G. Graphdiyne−ZnO Nanohybrids as an Advanced Photocatalytic Material. *J. Phys. Chem. C* **2015**, *119*, 22057−22065.

(34) Li, J.; Gao, X.; Liu, B.; Feng, Q.; Li, X.-B.; Huang, M.-Y.; Liu, Z.; Zhang, J.; Tung, C.-H.; Wu, L.-Z. Graphdiyne: A Metal-free Material as Hole Transfer Layer to Fabricate Quantum Dot-sensitized Photocathodes for Hydrogen Production. *J. Am. Chem. Soc.* **2016**, *138*, 3954−3957.

(35) Gao, X.; Zhou, J.; Du, R.; Xie, Z.; Deng, S.; Liu, R.; Liu, Z.; Zhang, J. Robust Superhydrophobic Foam: A Graphdiyne-based Hierarchical Architecture for Oil/water Separation. *Adv. Mater.* **2016**, *28*, 168−173.

(36) Jin, Z.; Zhou, Q.; Chen, Y.; Mao, P.; Li, H.; Liu, H.; Wang, J.; Li, Y. Graphdiyne: ZnO Nanocomposites for High-performance UV Photodetectors. *Adv. Mater.* **2016**, *28*, 3697−3702.

(37) Long, M.; Tang, L.; Wang, D.; Li, Y.; Shuai, Z. Electronic Structure and Carrier Mobility in Graphdiyne Sheet and Nanoribbons: Theoretical Predictions. *ACS Nano* **2011**, *5*, 2593−2600.

(38) Li, G.; Li, Y.; Qian, X.; Liu, H.; Lin, H.; Chen, N.; Li, Y. Construction of Tubular Molecule Aggregations of Graphdiyne for Highly Efficient Field Emission. *J. Phys. Chem. C* **2011**, *115*, 2611−2615.

(39) Qian, X.; Ning, Z.; Li, Y.; Liu, H.; Ouyang, C.; Chen, Q.; Li, Y. Construction of Graphdiyne Nanowires with High-conductivity and Mobility. *Dalton Trans.* **2012**, *41*, 730−733.

(40) Luo, G.; Zheng, Q.; Mei, W.-N.; Lu, J.; Nagase, S. Structural, Electronic, and Optical Properties of Bulk Graphdiyne. *J. Phys. Chem. C* **2013**, *117*, 13072−13079.

(41) Kuang, C.; Tang, G.; Jiu, T.; Yang, H.; Liu, H.; Li, B.; Luo, W.; Li, X.; Zhang, W.; Lu, F.; Fang, J.; Li, Y. Highly efficient electron transport obtained by doping PCBM with graphdiyne in planar-heterojunction perovskite solar cells. *Nano Lett.* **2015**, *15*, 2756−2762.

(42) Huang, C.; Li, Y. Structure of 2D graphdiyne and its application in energy fields. *Acta Phys.-Chim. Sin.* **2016**, *32*, 1314−1329.

(43) Huang, C.; Zhang, S.; Liu, H.; Li, Y.; Cui, G.; Li, Y. Graphdiyne for high capacity and long-life lithium storage. *Nano Energy* **2015**, *11*, 481−489.

(44) Li, Y.; Li, Y. Two Dimensional Polymers—Progress of full carbon graphyne. *Acta Polym. Sin.* **2015**, *2*, 147−165.

(45) Li, Y.; Liu, T.; Liu, H.; Tian, M.; Li, Y. Self-assembly of intramolecular charge-transfer compounds into functional molecular systems. *Acc. Chem. Res.* **2014**, *47*, 1186−1198.

(46) Li, Y.; Jia, Z.; Xiao, S.; Liu, H.; Li, Y. A method for controlling the synthesis of stable twisted two-dimensional conjugated molecules. *Nat. Commun.* **2016**, *7*, 11637.

(47) Xue, Y.; Guo, Y.; Yi, Y.; Li, Y.; Liu, H.; Li, D.; Yang, W.; Li, Y. Self-catalyzed growth of Cu@graphdiyne core−shell nanowires array for high efficient hydrogen evolution cathode. *Nano Energy* **2016**, DOI: 10.1016/j.nanoen.2016.09.005.

(48) Malko, D.; Neiss, C.; Viñes, F.; Görling, A. Competition for Graphene: Graphynes with Direction-dependent Dirac Cones. *Phys. Rev. Lett.* **2012**, *108*, 086804−086807.

(49) He, J.; Ma, S. Y.; Zhou, P.; Zhang, C. X.; He, C.; Sun, L. Z. Magnetic Properties of Single Transition-Metal Atom Absorbed Graphdiyne and Graphyne Sheet from DFT+U Calculations. *J. Phys. Chem. C* **2012**, *116*, 26313−26321.

(50) Jagadeesh, R. V.; Junge, H.; Pohl, M.-M.; Radnik, J.; Brückner, A.; Beller, M. Selective Oxidation of Alcohols to Esters using Heterogeneous Co_3O_4−N@C Catalysts under Mild Conditions. *J. Am. Chem. Soc.* **2013**, *135*, 10776−10782.

(51) Estrade-Szwarckopf, H. XPS Photoemission in Carbonaceous Materials: A "defect" Peak Beside the Graphitic Asymmetric Peak. *Carbon* **2004**, *42*, 1713−1721.

(52) Yan, X.; Xu, T.; Chen, G.; Yang, S.; Liu, H. Study of Structure, Tribological Properties and Growth Mechanism of DLC and Nitrogen-doped DLC Films Deposited by Electrochemical Technique. *Appl. Surf. Sci.* **2004**, *236*, 328−335.

(53) Wiggins-Camacho, J. D.; Stevenson, K. J. Effect of Nitrogen Concentration on Capacitance, Density of States, Electronic Conductivity, and Morphology of N-doped Carbon Nanotube Electrodes. *J. Phys. Chem. C* **2009**, *113*, 19082−19090.

(54) Liu, R.; Liu, H.; Li, Y.; Shang, X.; Zhang, S.; Yu, X.; Zhang, S.; Cao, H.; Zhang, G. Nitrogen-doped graphdiyne as a metal-free catalyst for high-performance oxygen reduction reactions. *Nanoscale* **2014**, *6*, 11336−11343.

(55) Haley, M. M. Synthesis and Properties of Annulenic Subunits of Graphyne and Graphdiyne Nanoarchitectures. *Pure Appl. Chem.* **2008**, *80*, 519−532.

(56) Luo, G.; Qian, X.; Liu, H.; Qin, R.; Zhou, J.; Li, L.; Gao, Z.; Wang, E.; Mei, W.-N.; Lu, J.; Li, Y.; Nagase, S. Quasiparticle Energies and Excitonic Effects of the Two-dimensional Carbon Allotrope

Graphdiyne: Theory and Experiment. *Phys. Rev. B: Condens. Matter Mater. Phys.* **2011**, *84*, 075439.

(57) Pan, Y.; Wang, Y.; Wang, L.; Zhong, H.; Quhe, R.; Ni, Z.; Ye, M.; Mei, W.-N.; Shi, J.; Guo, W.; Yang, J.; Lu, J. Graphdiyne-metal Contacts and Graphdiyne Transistors. *Nanoscale* **2015**, *7*, 2116−2127.

(58) Ferrari, A. C.; Robertson, J. Interpretation of Raman Spectra of Disordered and Amorphous Carbon. *Phys. Rev. B: Condens. Matter Mater. Phys.* **2000**, *61*, 14095−14107.

(59) Lado, J. L.; Wang, X.; Paz, E.; Carbó-Argibay, E.; Guldris, N.; Rodríguez-Abreu, C.; Liu, L.; Kovnir, K.; Kolen'ko, Y. V. Design and synthesis of highly active Al−Ni−P foam electrode for hydrogen evolution reaction. *ACS Catal.* **2015**, *5*, 6503−6508.

(60) Li, J.; Li, J.; Zhou, X.; Xia, Z.; Gao, W.; Ma, Y.; Qu, Y. Highly efficient and robust Nickel phosphides as bifunctional electrocatalysts for overall water-splitting. *ACS Appl. Mater. Interfaces* **2016**, *8*, 10826−10834.

(61) Hou, Y.; Lohe, M. R.; Zhang, J.; Liu, S.; Zhuang, X.; Feng, X. Vertically Oriented Cobalt Selenide/NiFe Layered-double-hydroxide Nanosheets Supported on Exfoliated Graphene Foil: an Efficient 3D Electrode for Overall Water Splitting. *Energy Environ. Sci.* **2016**, *9*, 478−483.

(62) Liu, D.; Lu, Q.; Luo, Y.; Sun, X.; Asiri, A. M. $NiCo_2S_4$ Nanowires Array as an Efficient Bifunctional Electrocatalyst for Full Water Splitting with Superior Activity. *Nanoscale* **2015**, *7*, 15122−15126.

(63) Ma, L.; Hu, Y.; Chen, R.; Zhu, G.; Chen, T.; Lv, H.; Wang, Y.; Liang, J.; Liu, H.; Yan, C.; Zhu, H.; Tie, Z.; Jin, Z.; Liu, J. Self-assembled Ultrathin $NiCo_2S_4$ Nanoflakes Grown on Ni Foam as High-performance Flexible Electrodes for Hydrogen Evolution Reaction in Alkaline Solution. *Nano Energy* **2016**, *24*, 139−147.

(64) Feng, J.-X.; Ding, L.-X.; Ye, S.-H.; He, X.-J.; Xu, H.; Tong, Y.-X.; Li, G.-R. $Co(OH)_2$@PANI Hybrid Nanosheets with 3D Networks as High-Performance Electrocatalysts for Hydrogen Evolution Reaction. *Adv. Mater.* **2015**, *27*, 7051−7057.

(65) Sehgal, A.; Lu, D.; Frankel, G. S. Pitting in Aluminum Thin Films: Supersaturation and Effects of Dichromate Ions. *J. Electrochem. Soc.* **1998**, *145*, 2834−2840.

(66) Kanan, M. W.; Nocera, D. G. In Situ Formation of an Oxygen-Evolving Catalyst in Neutral Water Containing Phosphate and Co^{2+}. *Science* **2008**, *321*, 1072−1075.

(67) Feng, L.-L.; Yu, G.; Wu, Y.; Li, G.-D.; Li, H.; Sun, Y.; Asefa, T.; Chen, W.; Zou, X. High-Index Faceted Ni_3S_2 Nanosheet Arrays as Highly Active and Ultrastable Electrocatalysts for Water Splitting. *J. Am. Chem. Soc.* **2015**, *137*, 14023−14026.

(68) Pentland, N.; Bockris, J. O. M.; Sheldon, E. Hydrogen Evolution Reaction on Copper, Gold, Molybdenum, Palladium, Rhodium, and Iron: Mechanism and Measurement Technique under High Purity Conditions. *J. Electrochem. Soc.* **1957**, *104*, 182−194.